

The N-Terminal Methionine of Cellular Proteins as a Degradation Signal

Heon-Ki Kim,^{1,3} Ryu-Ryun Kim,^{1,3} Jang-Hyun Oh,² Hanna Cho,¹ Alexander Varshavsky,^{2,*} and Cheol-Sang Hwang^{1,*}

¹Department of Life Sciences, Pohang University of Science and Technology, Pohang, Gyeongbuk 790-784, South Korea

²Division of Biology and Biological Engineering, California Institute of Technology, Pasadena, CA 91125, USA

³These authors contributed equally to this work

*Correspondence: avarsh@caltech.edu (A.V.), cshwang@postech.ac.kr (C.-S.H.)

<http://dx.doi.org/10.1016/j.cell.2013.11.031>

SUMMARY

The Arg/N-end rule pathway targets for degradation proteins that bear specific unacetylated N-terminal residues while the Ac/N-end rule pathway targets proteins through their N^ε-terminally acetylated (Nt-acetylated) residues. Here, we show that Ubr1, the ubiquitin ligase of the Arg/N-end rule pathway, recognizes unacetylated N-terminal methionine if it is followed by a hydrophobic residue. This capability of Ubr1 expands the range of substrates that can be targeted for degradation by the Arg/N-end rule pathway because virtually all nascent cellular proteins bear N-terminal methionine. We identified Msn4, Sry1, Arl3, and Pre5 as examples of normal or misfolded proteins that can be destroyed through the recognition of their unacetylated N-terminal methionine. Inasmuch as proteins bearing the Nt-acetylated N-terminal methionine residue are substrates of the Ac/N-end rule pathway, the resulting complementarity of the Arg/N-end rule and Ac/N-end rule pathways enables the elimination of protein substrates regardless of acetylation state of N-terminal methionine in these substrates.

INTRODUCTION

The N-end rule pathway recognizes proteins containing N-terminal degradation signals called N-degrons, polyubiquitylates these proteins and thereby causes their degradation by the proteasome (Bachmair et al., 1986; Varshavsky, 2011). The main determinant of an N-degron is a destabilizing N-terminal residue of a protein. Recognition components of the N-end rule pathway are called N-recognins. In eukaryotes, N-recognins are E3 ubiquitin (Ub) ligases that can target N-degrons (Figure S1 available online).

Regulated degradation of proteins or their fragments by the N-end rule pathway mediates a strikingly broad range of biological functions, including the sensing of heme, nitric oxide, and oxygen; the control, through degradation, of subunit stoichiometries in multisubunit proteins; the elimination of misfolded proteins; the repression of apoptosis and neurodegeneration; the

regulation of chromosome repair, transcription, replication, and cohesion/segregation; the regulation of G proteins, autophagy, peptide import, meiosis, immunity, fat metabolism, cell migration, actin filaments, cardiovascular development, spermatogenesis, neurogenesis, and memory; and the regulation of many processes in plants (Figure S1 and references therein) (Dogan et al., 2012; Finley et al., 2012; Tasaki et al., 2012; Varshavsky, 2008, 2011).

In eukaryotes, the N-end rule pathway consists of two branches. One of them, called the Arg/N-end rule pathway, targets specific unacetylated N-terminal residues (Figure S1B) (Bachmair et al., 1986; Brower et al., 2013; Piatkov et al., 2012a). N-terminal Arg, Lys, His, Leu, Phe, Tyr, Trp, and Ile are directly recognized by N-recognins. In contrast, N-terminal Asn, Gln, Asp, and Glu (as well as Cys, under some metabolic conditions) are destabilizing owing to their preliminary enzymatic modifications, which include N-terminal deamidation (Nt-deamidation) and Nt-arginylation (Figures S1B and S1C). In the yeast *S. cerevisiae*, the Arg/N-end rule pathway is mediated by the Ubr1 N-recognin, a 225 kDa RING-type E3 Ub ligase and a part of the targeting complex containing the Ubr1-Rad6 and Ufd4-Ubc4/5 holoenzymes (Hwang et al., 2010a).

The other branch, called the Ac/N-end rule pathway, recognizes proteins through their N^ε-terminally acetylated (Nt-acetylated) residues (Figure S1A) (Hwang et al., 2010b; Shemorry et al., 2013). The corresponding degradation signals and E3 Ub ligases are called Ac/N-degrons and Ac/N-recognins, respectively. Nt-acetylation of cellular proteins is apparently irreversible, in contrast to acetylation-deacetylation of internal Lys residues. The bulk of Nt-acetylation is cotranslational, being mediated by ribosome-associated Nt-acetylases. Approximately 90% of human proteins are Nt-acetylated (Arnesen et al., 2009; Mischerikow and Heck, 2011). Many, possibly most, Nt-acetylated proteins contain Ac/N-degrons (Figure S1A) (Hwang et al., 2010b; Shemorry et al., 2013).

Natural Ac/N-degrons are regulated through their steric shielding. A protein containing an Ac/N-degron is short lived unless it can repress (shield) its Ac/N-degron through intramolecular folding or interactions with other proteins (Figure 7A). The resulting hiatus from being vulnerable to degradation can be either long-lasting or transient, depending on the in vivo dynamics (dissociation-reconstitution) of a complex that sequesters the protein's Ac/N-degron (Shemorry et al., 2013). The cotranslational creation of Ac/N-degrons, their exceptional

prevalence, and their conditionality underlie the regulation, by the Ac/N-end rule pathway, of the input stoichiometries of subunits in multisubunit complexes, as well as the elimination of misfolded or otherwise abnormal proteins that cannot shield their Ac/N-degrons (Shemorry et al., 2013).

This understanding left open the question of what happens when the Nt-acetylation of a specific protein is incomplete. Many cellular proteins are partially Nt-acetylated, i.e., a protein can exist in vivo as a mix of Nt-acetylated and non-Nt-acetylated species (Arnesen et al., 2009). The unacetylated fraction of an incompletely Nt-acetylated protein would be invisible to the Ac/N-end rule pathway. Might there be a system that can gauge and control, through conditional proteolysis, the homeostasis of both Nt-acetylated proteins and their unacetylated counterparts?

Nascent polypeptides bear N-terminal methionine (Met), encoded by the AUG initiation codon. Ribosome-associated Met-aminopeptidases cotranslationally cleave off the N-terminal Met if a residue at position 2, to be made N terminal by the cleavage, is sufficiently small, i.e., if it is Gly, Ala, Ser, Thr, Cys, Pro, or Val (Xiao et al., 2010). The resulting N-terminal Ala, Ser, and Thr, as well as the retained N-terminal Met residue are often Nt-acetylated (Starheim et al., 2012). Other N-terminal residues are Nt-acetylated either less frequently or almost never (Figure S2A).

Until the present work, the unacetylated N-terminal Met was classed as a “stabilizing” (i.e., nondestabilizing) residue (Varshavsky, 2011). We show here that the *S. cerevisiae* Ubr1 N-recognin and its mouse counterparts Ubr1 and Ubr2 have the previously unknown ability to recognize proteins bearing the unacetylated N-terminal Met if the residue at position 2 is Leu, Phe, Tyr, Trp, Ile, Val or Ala, i.e., a non-Met hydrophobic (Φ) residue. Because Ala2 and Val2 allow the removal of N-terminal Met by Met-aminopeptidases (Xiao et al., 2010), the retention of Met requires a large second-position Φ residue, i.e., Leu, Phe, Tyr, Trp or Ile. Proteins containing this motif, termed Met- Φ proteins, are shown here to be short-lived substrates of both the Arg/N-end rule and Ac/N-end rule pathways.

The substrate range of the Ac/N-end rule pathway is exceptionally broad, as ~90% of human proteins are Nt-acetylated and many Nt-acetylated proteins contain Ac/N-degrons (Figure S1A) (Hwang et al., 2010b; Shemorry et al., 2013). The substrate range of the Arg/N-end rule pathway was thought to be much narrower, because the exposure of the previously known unacetylated destabilizing N-terminal residues in substrates of this pathway (Figure S1B) requires preliminary cleavages of proteins by nonprocessive proteases that include calpains, caspases, separases, and secretases. The discovery that this proteolytic system can target unacetylated Met- Φ proteins greatly expands the substrate range of the Arg/N-end rule pathway.

We found that the natural Met- Φ proteins Msn4, Sry1, Arl3, and Pre5 bear unacetylated Met-based N-degrons. We also found that the previously reported degradation of misfolded proteins by the Arg/N-end rule pathway (Eisele and Wolf, 2008; Heck et al., 2010) can involve the Ubr1-mediated recognition of these abnormal proteins through their Met-based N-degrons. The cited proteins are a part of an apparently much larger set of normal or misfolded proteins that can be destroyed through the recognition of their unacetylated N-terminal Met.

In either yeast or mammals, approximately 15% of genes encode Met- Φ proteins. As described below, many, possibly most, unacetylated Met- Φ proteins contain Met-based N-degrons. The resulting functional complementarity between the two branches of the N-end rule pathway makes possible the degradation-mediated control of Met- Φ proteins irrespective of the extent of their Nt-acetylation. Specifically, it is shown here that an Nt-acetylated Met- Φ protein can be destroyed by the Ac/N-end rule pathway while the otherwise identical unacetylated protein can be eliminated, independently, by the Arg/N-end rule pathway (Figures 6, 7, and S1).

RESULTS

Binding of N-Recognins to Met- Φ Peptides

First indications that *S. cerevisiae* Ubr1 has a broader than previously known recognition specificity were provided by peptide arrays on membrane support (SPOT). In these assays, XZ-e^{K(3-10)} peptides were C-terminally linked to a membrane in equal molar amounts and probed for binding to purified, flag-tagged *S. cerevisiae* Ubr1 (Sc^fUbr1) or to its mouse counterparts Mm^fUbr1 and Mm^fUbr2 (Figures 1A and 1B). The notation e^{K(3-10)} (extension [e] containing lysine [K]) denotes eight residues (after the varying residues X and Z) of the previously characterized ~40-residue e^K sequence upstream of engineered N-end rule reporters (Hwang et al., 2010b; Varshavsky, 2011).

Sc^fUbr1 was found to bind to unacetylated Met-Z-e^{K(3-10)} peptides in which Z = Ala, Val, Leu, Ile, Phe, Trp, Tyr (Figure 1A, spots 1, 5, 8, 10, 18-20), but did not significantly bind to the otherwise identical Met-Z-e^{K(3-10)} peptides in which Z = Cys, Asp, Glu, Gly, His, Lys, Met, Asn, Pro, Gln, Arg, Ser, Thr (Figure 1A, spots 2-4, 6, 7, 9, 11-17). In agreement with these data, a SPOT assay with Sc^fUbr1 as well as mouse Mm^fUbr1 and Mm^fUbr2 showed that yeast Ubr1 could bind to Met-Leu-e^{K(3-10)} but not to Met-Lys-e^{K(3-10)} (with Lys at position 2) and that the binding patterns of mouse Ubr1 and Ubr2 were similar to those of yeast Ubr1, including the absence of binding to Nt-acetylated counterparts of the unacetylated peptides (Figure 1B).

Given the pattern of retention of N-terminal Met in nascent proteins (see Introduction), the SPOT results suggested that Ubr1 can target proteins in vivo through their retained unacetylated N-terminal Met if it is followed by one of the large Φ residues Leu, Phe, Tyr, Trp, or Ile. We show, below, that this is indeed the case. The corresponding degrons of Met- Φ and AcMet- Φ proteins were termed Met ^{Φ} /N-degrons and AcMet ^{Φ} /N-degrons, respectively.

Degradation of Met- Φ Proteins by the Arg/N-End Rule Pathway

The 35 kDa Met-Z-e^K-ha-Ura3 (MZ-Ura3) reporters comprised N-terminal Met, a varying residue Z at position 2, the e^K extension (see above), the ha epitope, and *S. cerevisiae* Ura3. MZ-Ura3 proteins were produced through the cotranslational deubiquitylation of Ub-MZ-Ura3, expressed in yeast using low copy plasmids and the P_{CUP1} promoter (Hwang et al., 2010b).

We showed previously that ML-Ura3 in wild-type (WT) cells was at least partially Nt-acetylated in vivo by the NatC Nt-acetylase and that the resulting AcML-Ura3 was targeted for degradation by the Ac/N-end rule pathway (Figures S1A and

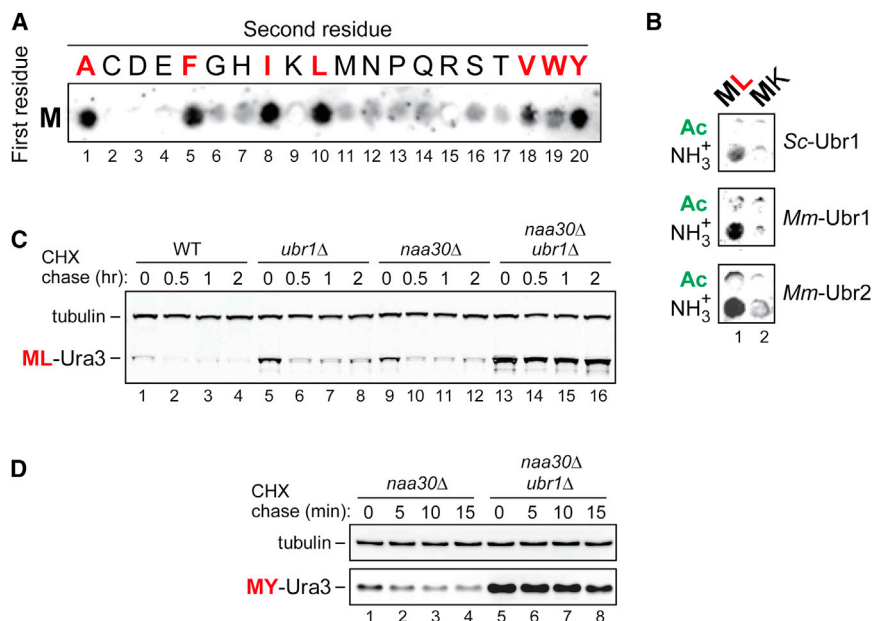


Figure 1. Specific Binding of Ubr1 to Unacetylated N-Terminal Methionine Followed by a Hydrophobic Residue

(A) SPOT assay with *S. cerevisiae* ^fUbr1 and Met-Z-e^{K(3-10)} peptides MZGSGAWLLP (Z = Ala, Cys, Asp, Glu, Phe, Gly, His, Ile, Lys, Leu, Met, Asn, Pro, Gln, Arg, Ser, Thr, Val, Trp, Tyr).

(B) Same as in A but with *S. cerevisiae* ^fUbr1 (Sc^fUbr1), mouse ^fUbr1 (Mm^fUbr1) and mouse ^fUbr2 (Mm^fUbr2) versus Met-Z-e^{K(3-10)} (Z = Leu, Lys) peptides and their Nt-acetylated counterparts.

(C) Cycloheximide (CHX) chases with ML-Ura3 in WT (lanes 1–4), *ubr1*Δ (lanes 5–8), *naa30*Δ (lanes 9–12), and *naa30*Δ *ubr1*Δ cells (lanes 13–16).

(D) CHX chases with MY-Ura3 in *naa30*Δ (lanes 1–4) and *naa30*Δ *ubr1*Δ cells (lanes 5–8). See also Figures S1, S2, and S3.

S2A) (Hwang et al., 2010b). Cycloheximide (CHX) chases indicated that the short-lived ML-Ura3 was longer lived in *ubr1*Δ cells (lacking the Arg/N-end rule pathway) and in *naa30*Δ (*mak3*Δ) cells (lacking the NatC Nt-acetylase) (Figures 1C and S2B). Moreover, ML-Ura3 was synergistically and nearly completely stabilized, in addition to a further increase of its prechase level, in *naa30*Δ *ubr1*Δ cells (Figure 1C). In contrast to pulse-chase assays, CHX-chases do not distinguish between “young” and “old” protein molecules. ³⁵S-pulse-chases with ML-Ura3 (expressed from Ub-ML-Ura3 or directly as ML-Ura3) yielded results similar to those with CHX-chases (Figure 1C), including higher prechase levels of ³⁵S-pulse-labeled ML-Ura3 in *naa30*Δ *ubr1*Δ cells versus *naa30*Δ cells (Figure S3A–S3D).

The CHX-chase patterns with MI-Ura3 and MY-Ura3, in which Leu2 was replaced by other Φ residues, Ile, or Tyr, were similar to those with ML-Ura3. Specifically, MI-Ura3 and MY-Ura3 were short lived in *naa30*Δ cells but became nearly completely stable in *naa30*Δ *ubr1*Δ cells, with striking increases in their prechase levels (Figures 1D, 2A, and 2C).

The unacetylated state of ML-Ura3 in *naa30*Δ cells (Hwang et al., 2010b), the binding of Ubr1 to unacetylated N-terminal Met-Φ sequences (Figures 1A and 1B), and the synergistic stabilization of ML-Ura3, MI-Ura3, and MY-Ura3 by the ablation of both Ubr1 and NatC in *naa30*Δ *ubr1*Δ cells (Figures 1C, 1D, 2A, 2C, and S3A–S3D) indicated that these reporters were destroyed through their Met^Φ/N-degrons in *naa30*Δ cells. In an independent support of this conclusion, and in striking contrast to the instability of ML-Ura3, MI-Ura3, and MY-Ura3 in *naa30*Δ cells, the otherwise identical MK-Ura3, containing Lys2 (instead of Leu2 in ML-Ura3), was long lived in *naa30*Δ cells under the same conditions (Figures 2B and 2D). Moreover, the prechase level of MK-Ura3 was ~5-fold higher than that of ML-Ura3 (Figures 2B and 2D). These in vivo results were predicted by in vitro data, as there was no significant binding of Ubr1 to N-terminal Met if position 2 was occupied by a basic residue such as Lys (Figures 1A and 1B).

RT-PCR of mRNA encoding ML-Ura3 indicated no significant changes in the level of this mRNA between *naa30*Δ cells and *naa30*Δ *ubr1*Δ cells (Figure S4C), in striking contrast to the considerably higher levels of the ML-Ura3 protein (and of the analogous MI-Ura3 and MY-Ura3) both before and during CHX-chases in *naa30*Δ *ubr1*Δ cells (Figures 1C, 1D, 2A, and 2C). Thus, the observed increases of protein levels stemmed either largely or entirely from changes in the rate of degradation of these proteins.

A Binding Site of Ubr1 That Recognizes Met^Φ/N-Degrans

The ~80-residue UBR domain of the 1,950-residue Ubr1 contains its type 1 binding site, which recognizes the N-terminal basic residues Arg, Lys, or His (Choi et al., 2010; Matta-Camacho et al., 2010). The nearby type-2 binding site of Ubr1 recognizes the large N-terminal Φ residues Leu, Phe, Tyr, Trp, or Ile (Figure 2F) (Xia et al., 2008). To map a site that recognizes the unacetylated N-terminal Met of Met-Φ proteins, we performed glutathione-S-transferase (GST)-pulldowns with purified ML-e^K-GST (ML-GST) and extracts from *S. cerevisiae* that expressed the flag-tagged full-length Ubr1¹⁻¹⁹⁵⁰ or its fragments ^fUBR¹⁻⁷¹⁷, ^fUBR^{209-1140f}, ^fUBR¹⁻³¹⁰, ^fUBR⁹⁸⁻⁵¹⁸, and ^fUBR²⁰⁹⁻⁷¹⁷. The ^fUBR¹⁻⁷¹⁷ fragment, which contained the type-1 and type-2 binding sites, could bind to ML-GST, but shorter N-terminal fragments of Ubr1 or its C-terminal fragments did not bind to ML-GST (Figures 2F–2I).

Dipeptides with type-1 or type-2 destabilizing N-terminal residues (Figure S1B) can inhibit, through competition, the binding of Ubr1 to proteins bearing these N-terminal residues (Varshavsky, 2011). We used the type 1 Arg-Ala and/or type 2 Leu-Ala dipeptides with the previously characterized, completely defined in vitro ubiquitylation system (Hwang et al., 2010a). It comprised purified Ub, the Uba1 E1 enzyme, the Rad6 E2 enzyme, the Ubr1 E3 N-recognin, and the unacetylated ML-GST reporter. Leu-Ala completely inhibited the Ubr1-dependent polyubiquitylation of ML-GST (Figure 2E, lanes 4 versus 2), whereas Arg-Ala enhanced its polyubiquitylation, without negating the inhibitory effect of Leu-Ala if the two dipeptides were added together

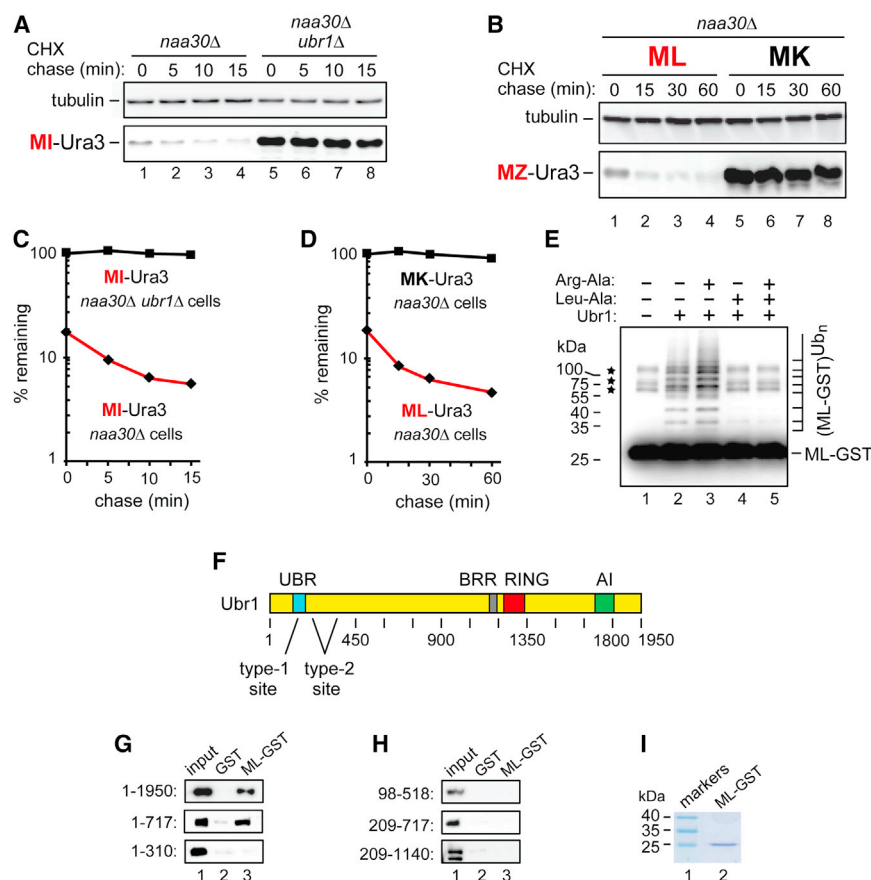


Figure 2. Unacetylated N-Terminal Methionine as an N-Degron of the Arg/N-End Rule Pathway

(A) CHX chases with MI-Ura3 in *naa30Δ* (lanes 1–4) and *naa30Δ ubr1Δ* cells (lanes 5–8). (B) CHX chases with ML-Ura3 (lanes 1–4) and MK-Ura3 (lanes 5–8) in *naa30Δ* cells. (C) Quantification of data in (A). (D) Quantification of data in (B). In (A)–(D), the corresponding CHX-chase assays were carried out at least three times and yielded results within 10% of the data shown. (E) In vitro polyubiquitylation of purified ML-GST by the purified Ubr1-Rad6 Ub ligase. Lane 1, complete assay but without Ubr1 (the asterisks indicate three minor contaminants in purified ML-GST, whose band is indicated on the right). Lane 2, same as lane 1 but with Ubr1. Lane 3, same as lane 2 but with Arg-Ala (1 mM). Lane 4, same as lane 2 but with Leu-Ala (1 mM). Lane 5, same as lane 2 but with Arg-Ala and Leu-Ala. (F) The UBR, BRR, RING, and AI regions of the *S. cerevisiae* Ubr1 N-recogin (Varshavsky, 2011). (G) GST-pulldown assays with ML-GST versus GST and either full-length Ubr1¹⁻¹⁹⁵⁰ or its fragments Ubr1¹⁻⁷¹⁷ and Ubr1¹⁻³¹⁰. (H) Same as in G but with Ubr1⁹⁸⁻⁵¹⁸, Ubr1²⁰⁹⁻⁷¹⁷, and Ubr1²⁰⁹⁻¹¹⁴⁰. (I) SDS-PAGE of purified ML-GST (lane 2). See also Figures S1, S2, S3, and S4.

(Figure 2E, lanes 3 versus 5). The positive allosteric effect of Arg-Ala was previously observed with other type 2 N-end rule substrates, whose binding to the type 2 site of Ubr1 was shown to be allosterically enhanced by the occupancy of its type 1 site (Varshavsky, 2011). Together, the ubiquitylation data and the pattern of ML-GST binding to Ubr1 and its fragments (Figures 2E–2I) strongly suggested that the recognition of N-terminal Met in Met- Φ proteins by Ubr1 is mediated by its previously characterized (Xia et al., 2008) type 2 binding site.

Degradation of a Misfolded Protein Through Its Met Φ /N-Degron

Studies by Wolf, Hampton, and colleagues showed that a variety of misfolded proteins can be destroyed by the Ubr1-dependent Arg/N-end rule pathway (Eisele and Wolf, 2008; Fredrickson and Gardner, 2012; Heck et al., 2010; Prasad et al., 2010; Summers et al., 2013; Theodoraki et al., 2012). One Ubr1 substrate of this class is the short-lived 110 kDa Δ ssC²²⁻⁵¹⁹Leu2_{myc}, comprising a misfolded PRC1-derived moiety, the Leu2 moiety, and the myc₁₃ tag (Eisele and Wolf, 2008). Because Δ ssC²²⁻⁵¹⁹Leu2_{myc} starts with Met-Ile (a Met- Φ sequence), we asked whether this protein, denoted as MI- Δ ssC²²⁻⁵¹⁹Leu2_{myc}, was targeted through its N-terminal Met.

CHX-chases of MI- Δ ssC²²⁻⁵¹⁹Leu2_{myc} showed it to be short lived in WT cells and significantly stabilized in *ubr1Δ* cells (Figures 3A and 3D), in agreement with earlier findings (Eisele and

Wolf, 2008). MI- Δ ssC²²⁻⁵¹⁹Leu2_{myc} was stabilized in double-mutant *naa30Δ ubr1Δ* cells even stronger than in *ubr1Δ* cells, with a further increase of its prechase level (Figures 3A and 3D). MI- Δ ssC²²⁻⁵⁸Ura3_{ha}, containing the first 37 residues of the Δ ssC²²⁻⁵¹⁹ moiety, the Ura3 moiety, and the ha tag, was also short lived in WT cells, and was strikingly stabilized in *ubr1Δ* cells (Figures 3B and 3E).

Given the presence of Ubr1-dependent Met Φ /N-degrons in MZ-Ura3 proteins (Figures 1C, 1D, and 2A–2D), the results with MI- Δ ssC²²⁻⁵¹⁹Leu2_{myc} and MI- Δ ssC²²⁻⁵⁸Ura3_{ha} (Figures 3A, 3B, and 3D) indicated that these proteins were destroyed largely through their Met Φ /N-degrons. If so, the Ile2→Lys2 mutation should abrogate this degradation in WT cells, because Ubr1 does not bind to N-terminal Met-Lys (Figures 1A and 1B). Indeed, MK- Δ ssC²²⁻⁵⁸Ura3_{ha} was completely stable in WT cells, in striking contrast to the degradation of the otherwise identical MI- Δ ssC²²⁻⁵⁸Ura3_{ha} (Figure 3C). In sum, at least some misfolded Met- Φ proteins, including MI- Δ ssC²²⁻⁵¹⁹Leu2_{myc} and MI- Δ ssC²²⁻⁵⁸Ura3_{ha}, are destroyed by the Arg/N-end rule pathway through their Met Φ /N-degrons.

Met Φ /N-Degrans and AcMet Φ /N-Degrans in Natural Proteins

The findings so far indicated the following mode of degradation of a Met- Φ protein (Figures 1, 2, and 3):

- (1) The unacetylated N-terminal Met of a Met- Φ protein can act as a Met Φ /N-degion, leading to the degradation of

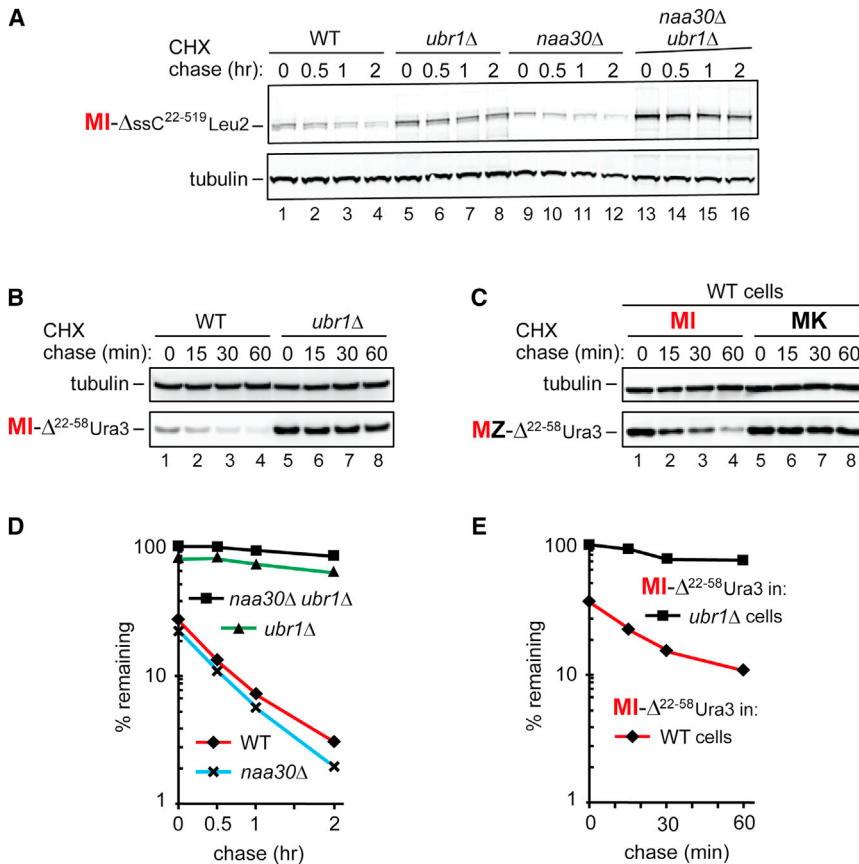


Figure 3. Misfolded Proteins Containing Met-Based N-Degrans

(A) CHX chases with MI-ΔssC²²⁻⁵¹⁹Leu2_{myc} in WT (lanes 1–4), *ubr1*Δ (lanes 5–8), *naa30*Δ (lanes 9–12), and *naa30*Δ *ubr1*Δ cells (lanes 13–16).

(B) CHX-chases with MI-ΔssC²²⁻⁵⁸Ura3_{ha} in WT (lanes 1–4) and *ubr1*Δ cells (lanes 5–8).

(C) CHX-chases with MI-ΔssC²²⁻⁵⁸Ura3_{ha} (lanes 1–4) and MK-ΔssC²²⁻⁵⁸Ura3_{ha} (lanes 5–8) in WT cells.

(D) Quantification of data in (A).

(E) Quantification of data in (B).

In (A)–(E), the corresponding CHX-chase assays were carried out at least three times and yielded results within 10% of the data shown. See also Figures S1 and S2.

Msn4

The 70 kDa Msn4 (N terminus: MLV–), denoted as ML-Msn4_{ha}, is a short-lived transcriptional activator that induces specific genes in response to stresses (Takatsume et al., 2010). ML-Msn4_{ha} was a highly unstable protein ($t_{1/2} \ll 1$ hr) in WT cells (Figures 4A and 4B). ML-Msn4_{ha} was partially stabilized in *ubr1*Δ cells, indicating the presence of Met^Φ/N-degron in some molecules of ML-Msn4_{ha} in WT cells (Figures 4A and 4B). ML-Msn4_{ha} was more strongly but still partially stabilized in *naa30*Δ cells, indicating the presence of AcMet^Φ/N-

degron in other (Nt-acetylated) molecules of ML-Msn4_{ha} in WT cells (Figures 4A and 4B).

In a most telling pattern analogous to but even more striking than the results with engineered MZ-Ura3 proteins (Figures 1C, 1D, and 2A–2D), ML-Msn4_{ha} was synergistically stabilized in *naa30*Δ *ubr1*Δ cells (Figure 4A, lanes 10–12 versus 1–3, and Figure 4B). Remarkably, the prechase level of ML-Msn4_{ha} in *naa30*Δ *ubr1*Δ cells was at least 30-fold higher than in WT cells (Figures 4A and 4B). Despite this enormous increase, ML-Msn4_{ha} retained a part of its instability in double-mutant cells, suggesting the presence of an internal degron as well (Figures 4A and 4B).

Independent evidence that the unacetylated ML-Msn4_{ha} was degraded by the Arg/N-end rule pathway in NatC-lacking *naa30*Δ cells was provided by the Leu2 → Lys2 mutation, which stabilized the resulting MK-Msn4_{ha}, in addition to strikingly increasing its prechase level (Figures 4C and 4D). These in vivo results were predicted by the in vitro evidence that Ubr1 does not bind to N-terminal Met-Lys (Figures 1A and 1B).

Sry1

The 35 kDa Sry1 (N terminus: MIV–), denoted as MI-Sry1, is a 3-hydroxyaspartate dehydratase. It modifies 3-hydroxyaspartate, a potentially toxic microbial metabolite (Wada et al., 2003). We produced MI-Sry1 in two ways, either as MI-Sry1_{ha3}, expressed from the native P_{SRY1} promoter and the endogenous (chromosomal) SRY1 locus instead of WT MI-Sry1, or as

this protein by the Ubr1-dependent Arg/N-end rule pathway.

- (2) Nt-acetylation converts a Met^Φ/N-degron into AcMet^Φ/N-degron and thereby shifts the targeting of the resulting AcMet^Φ protein to the Ac/N-end rule pathway.

The dual-pathway circuit that is revealed by this understanding (Figures 6 and 7) comprises the Nt-acetylated AcMet^Φ protein, the at least transient presence of its unacetylated Met^Φ counterpart, and the targeting of these otherwise identical proteins by two mechanistically distinct branches of the N-end rule pathway. An unacetylated Met^Φ protein is vulnerable to the Arg/N-end rule pathway. However, at least some molecules of this protein would be irreversibly Nt-acetylated before their encounters with Ubr1. Nt-acetylation of these Met^Φ molecules would preclude their capture by Ubr1 while making them vulnerable to the Ac/N-end rule pathway (Figures 6 and 7). To begin exploring this deeper understanding, we chose the *S. cerevisiae* Met^Φ proteins Msn4, Sry1, Arl3, and Pre5 from hundreds of *S. cerevisiae* Met^Φ proteins. These partly random choices were determined largely by the fact that the cited proteins are Nt-acetylated in WT yeast (Arnesen et al., 2009). (Met^Φ proteins are expected to be at least partially Nt-acetylated by the NatC Nt-acetylase; Figure S2A.) The proteins were C-terminally ha-tagged and expressed from the P_{CUP1} promoter on a low copy plasmid.

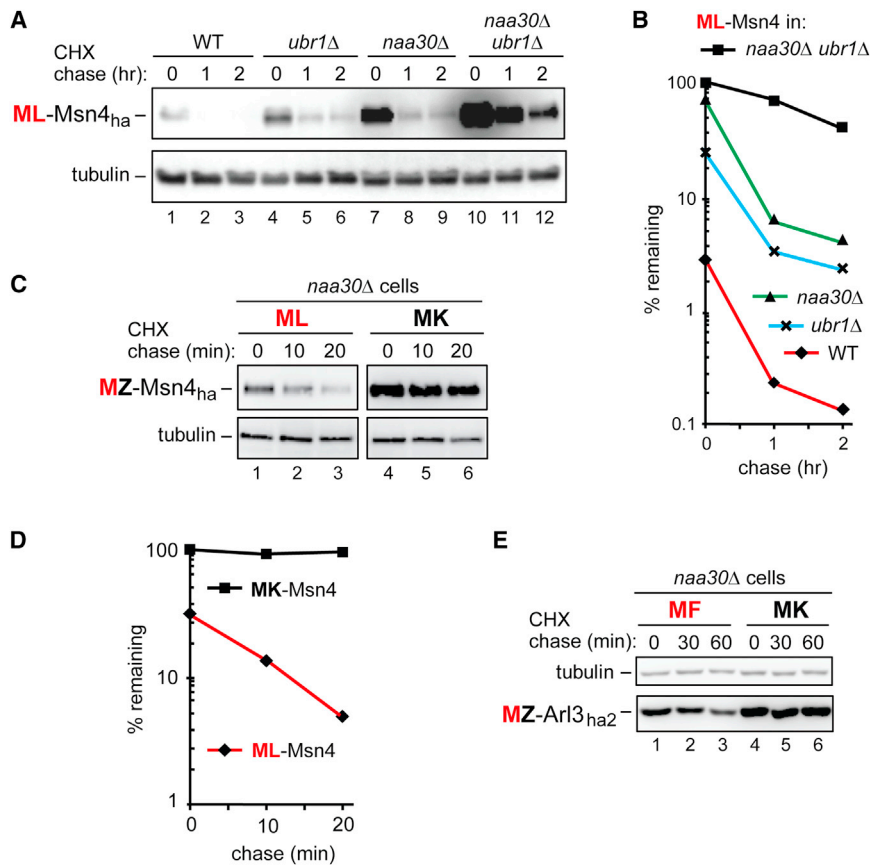


Figure 4. The Natural ML-Msn4 and MF-Arl3 Proteins Contain Met-Based N-Degrans

(A) CHX chases with ML-Msn4_{ha} in WT (lanes 1–3), *ubr1*Δ (lanes 4–6), *naa30*Δ (lanes 7–9), and *naa30*Δ *ubr1*Δ cells (lanes 10–12). (B) Quantification of data in (A). (C) CHX chases with ML-Msn4_{ha} (lanes 1–3) and MK-Msn4_{ha} (lanes 4–6) in *naa30*Δ cells. (D) Quantification of data in (C). (E) CHX chases with MF-Arl3_{ha2} (lanes 1–3) and MK-Arl3_{ha2} (lanes 4–6) in *naa30*Δ cells. In (A)–(E), the corresponding CHX-chase assays were carried out at least three times and yielded results within 10% of the data shown. See also Figures S1 and S2.

dence that Ubr1 does not bind to N-terminal Met-Lys (Figures 1A and 1B).

Arl3

The 22 kDa Arl3 (N terminus: MFH-), denoted as MF-Arl3_{ha2}, is a Golgi-associated cytosolic GTPase. Nt-acetylation of Arl3 is required for its targeting to Golgi (Behnia et al., 2004; Setty et al., 2004). MF-Arl3_{ha2} was unstable ($t_{1/2}$ ~35 min) in *naa30*Δ cells (Figure 4E). Given the results with other Met-Φ proteins (Figures 1, 2, 3, 4, 5), the unacetylated (in *naa30*Δ cells) N-terminal Met-Phe of MF-Arl3_{ha2} was expected to be targeted by the Arg/N-end rule pathway (Figure 6). If so,

the Phe2→Lys2 mutation in MF-Arl3_{ha2} should abrogate this degradation. Indeed, MK-Arl3_{ha2} was completely stable during CHX-chase in *naa30*Δ cells, in contrast to MF-Arl3_{ha2} (Figure 4E). Similarly to the findings with MZ-Ura3, MZ-ΔssC^{22–58}-Ura3_{ha}, MZ-Msn4_{ha}, and MZ-Sry1_{ha} (Figures 2B, 2D, 3C, 3F, 4C, 4D, and 5C), this in vivo result was predicted by the in vitro data about the absence of Ubr1 binding to N-terminal Met-Lys (Figure 1A and 1B). In sum, the unacetylated MF-Arl3_{ha2} contains a Met^Φ/N-degron.

Pre5

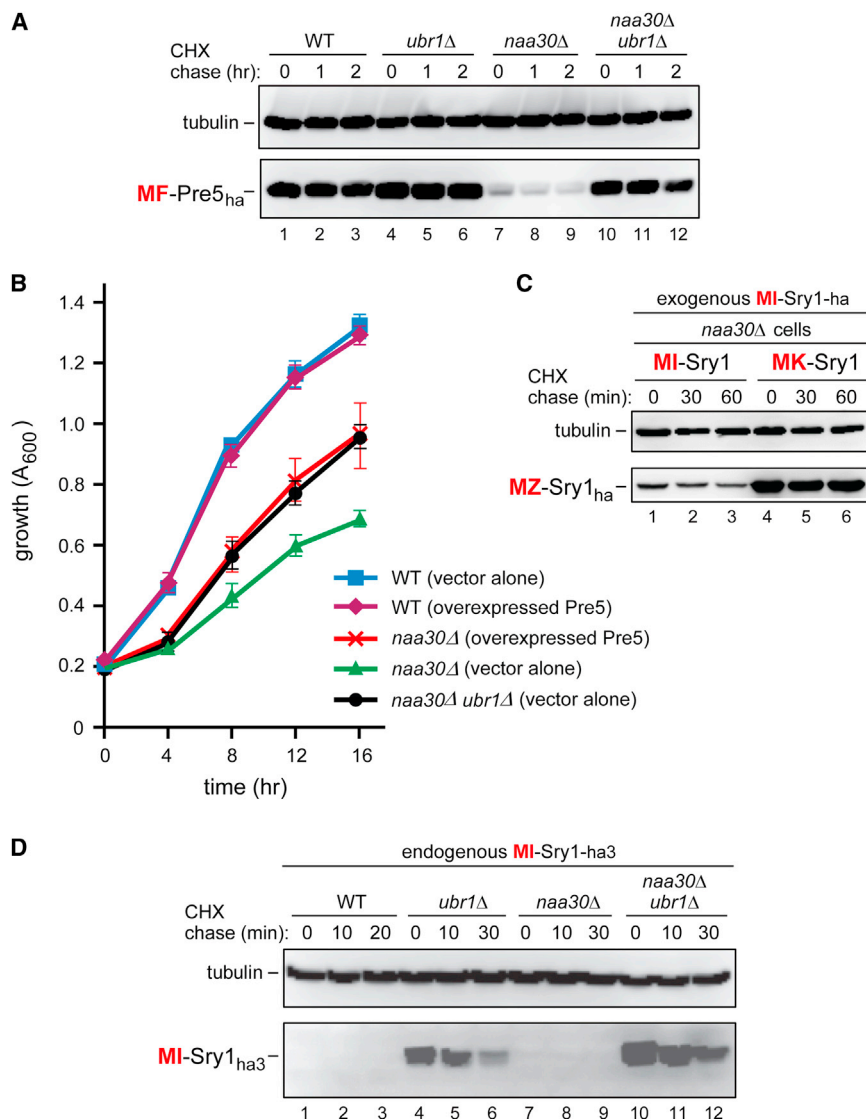
The 25 kDa Pre5 (N terminus: MFR-), denoted as MF-Pre5_{ha}, is a subunit of the 20S proteasome (Heinemeyer et al., 1994). MF-Pre5_{ha} was a relatively long-lived protein in WT cells ($t_{1/2}$ > 1 hr), in *ubr1*Δ cells, and in *naa30*Δ *ubr1*Δ cells (Figure 5A, lanes 1–3 versus lanes 4–6 and 10–12). Remarkably, however, MF-Pre5_{ha} became so short lived in *naa30*Δ cells (lacking the NatC Nt-acetylase) that it was barely detectable even before the chase (Figure 5A, lanes 7–9 versus 1–3). An illuminating explanation of this striking effect is described in Discussion. ³⁵S-pulse-chases of MF-Pre5_{ha} were in agreement with CHX-chase results in that MF-Pre5_{ha} was unstable in *naa30*Δ cells and was stabilized in *naa30*Δ *ubr1*Δ cells, including its strongly increased prechase level (Figures S4A and S4B).

RT-PCR of mRNAs encoding ML-Ura3, MI-Sry1, and MF-Pre5 indicated no significant changes in the level of these mRNAs between *naa30*Δ cells and *naa30*Δ *ubr1*Δ cells (Figures S4C–S4F),

MI-Sry1_{ha}, moderately overexpressed from the *P*_{CUP1} promoter on a low copy plasmid in Sry1⁺ cells. Analyzed by CHX-chases, the level of exogenously expressed MI-Sry1_{ha} was low in WT cells and even lower in *naa30*Δ cells, in which MI-Sry1_{ha} was not Nt-acetylated. Tellingly, the levels of MI-Sry1_{ha} were strikingly (more than 25-fold) higher in either *ubr1*Δ or *naa30*Δ *ubr1*Δ cells than in WT or *naa30*Δ cells (Figure S3E). ³⁵S-pulse-chases of exogenously expressed MI-Sry1_{ha} in *naa30*Δ cells versus *naa30*Δ *ubr1*Δ cells were in agreement with CHX-chase results in that pulse-labeled MI-Sry1_{ha} was unstable in *naa30*Δ cells and was stabilized in *naa30*Δ *ubr1*Δ cells, including its strongly increased prechase level (Figures S3F and S3G).

In CHX-chases with the endogenous MI-Sry1_{ha3}, which was expressed from the *P*_{SRY1} promoter and the *SRY1* chromosomal locus, the level of MI-Sry1_{ha3} was too low for detection in either WT or *naa30*Δ cells, which lacked the cognate NatC Nt-acetylase (Figure 5D). Strikingly, however, and similarly to the exogenously expressed MI-Sry1_{ha}, the level of endogenous MI-Sry1_{ha3} became at least 20-fold higher in *ubr1*Δ cells before the chase and was even further increased in *naa30*Δ *ubr1*Δ cells (Figure 5D).

Independent evidence that the unacetylated MI-Sry1_{ha} was degraded by the Arg/N-end rule pathway in NatC-lacking *naa30*Δ cells was provided by the Ile2→Lys2 mutation. It stabilized the resulting MK-Sry1_{ha} and greatly increased its level before the chase (Figure 5C), in agreement with the in vitro evi-



in contrast to much higher levels of the corresponding proteins in *naa30Δ ubr1Δ* cells (Figures 1C, 1D, 2A, 2C, 5A, and 5D, and S3E–S3G). Thus, strong increases in the levels of these proteins stemmed either largely or entirely from changes in the rate of their degradation, particularly the one that occurred either cotranslationally or shortly afterward, in agreement with evidence for a significant degradation of nascent and newly formed proteins (Duttler et al., 2013; Hartl et al., 2011; Turner and Varshavsky, 2000; Wang et al., 2013; Yewdell et al., 2011).

Overexpression of Pre5 Rescues Growth of *naa30Δ* Cells but Is Unnecessary in *naa30Δ ubr1Δ* Cells

The instability of (unacetylated) MF-Pre5 in *naa30Δ* cells suggested that the previously unexplained slow-growth phenotype of *naa30Δ* cells (Starheim et al., 2012) might be caused, in part, by low levels of the normally abundant, in WT cells, but now unacetylated and short-lived MF-Pre5 proteasomal subunit, owing to its degradation by the Arg/N-end rule pathway. We

asked, therefore, whether overexpression of MF-Pre5 might partially rescue the slow growth of *naa30Δ* cells. Indeed, overexpression of MF-Pre5 (at 37°C, to increase the dependence of growth on the proteasome activity; Finley et al., 2012), was found to accelerate the growth of *naa30Δ* cells from ~50% to ~85% of the WT growth rate under the same conditions (Figure 5B). Remarkably, we also found that *naa30Δ ubr1Δ* cells, in the absence of MF-Pre5 overexpression, grew as fast as the “rescued” *naa30Δ* cells overexpressing MF-Pre5 (Figure 5B) (see Discussion).

DISCUSSION

The main discovery of this study revealed a link between the Ac/N-end rule pathway and the Arg/N-end rule pathway, two universally present pathways of protein degradation (Figures 6, 7 and S1). We found that the *S. cerevisiae* Ubr1 N-recognin of the

Figure 5. The Natural MF-Pre5 and MI-Sry1 Proteins Contain Met-Based N-Degrans

(A) CHX chases with MF-Pre5_{ha} in WT (lanes 1–3), *ubr1Δ* (lanes 4–6), *naa30Δ* (lanes 7–9), and *naa30Δ ubr1Δ* cells (lanes 10–12).

(B) Growth rates of WT, *naa30Δ* and *naa30Δ ubr1Δ* *S. cerevisiae* strains, including WT and *naa30Δ* strains that overexpressed the MF-Pre5 proteasomal subunit. Standard errors (of triplicate measurements) are shown as well.

(C) CHX chases with MI-Sry1_{ha} (lanes 1–3) and MK-Sry1_{ha} (lanes 4–6) in *naa30Δ* cells.

(D) CHX chases with endogenously expressed MI-Sry1_{ha} in WT (lanes 1–3), *ubr1Δ* (lanes 4–6), *naa30Δ* (lanes 7–9), and *naa30Δ ubr1Δ* cells (lanes 10–12).

See also Figures S1, S2, and S4.

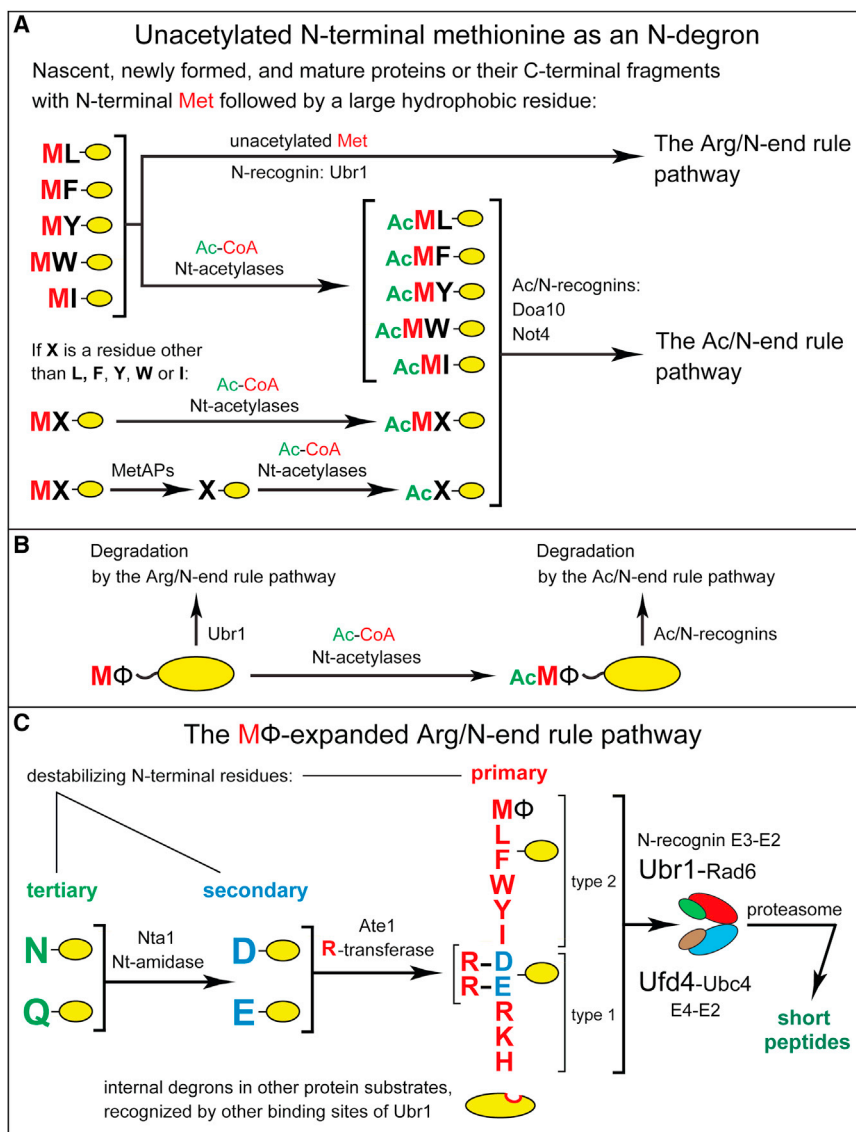


Figure 6. Complementary Specificities of the Arg/N-End Rule Pathway and the Ac/N-End Rule Pathway

(A) This diagram summarizes the main discovery of the present work, a functional complementarity between the Arg/N-end rule and Ac/N-end rule pathways. This complementarity stems from the recognition of the previously unknown Met^Φ/N-degrons in Met-Φ proteins versus the recognition of the previously characterized AcMet^Φ/N-degrons in AcMet-Φ proteins. AcMet^Φ/N-degrons are a subset of Ac/N-degrons in Nt-acetylated cellular proteins (Hwang et al., 2010b; Shemorry et al., 2013). Met-Φ proteins are defined, in this study, as those that bear N-terminal Met followed by a large hydrophobic (Φ) non-Met residue.

(B) Condensed summary of the dual-pathway circuit shown in A.

(C) The MΦ-based expansion of the Arg/N-end rule pathway in the present work, through the addition of a large set of new substrates, Met-Φ proteins.

See also Figure S1.

cant biological ramifications. Msn4 (transcriptional activator), Sry1 (3-hydroxyaspartate dehydratase), Arl3 (GTPase of the Ras superfamily), and Pre5 (proteasomal subunit) (Figures 4, 5, and S3) are the initial examples of natural Met-Φ proteins whose unacetylated N-terminal Met residues are shown here to function as Met^Φ/N-degrons. Many other proteins of the Met-Φ class are likely to be similar to Msn4, Sry1, Arl3, and Pre5 in their vulnerability to the Arg/N-end rule pathway (through their unacetylated N-terminal Met) and also, alternatively, to the Ac/N-end rule pathway, through their Nt-acetylated AcMet (Figures 6 and 7).

We also showed here that the misfolded protein ΔssC²²⁻⁵¹⁹Leu2^{myc}, a previously identified short-lived substrate of the Arg/N-end rule pathway (Eisele and Wolf, 2008), contains a Met^Φ/N-degron and is targeted by Ubr1 through this, previously unknown class of N-degrons (Figures 3, 6, and 7B). Given these results, it is likely that prematurely terminated (truncated) polypeptides of the Met-Φ class can also be targeted by the Arg/N-end rule pathway through their Met^Φ/N-degrons or, alternatively, by the Ac/N-end rule pathway through their AcMet^Φ/N-degrons. It remains to be determined whether the degradation of other misfolded Met-Φ proteins is mediated by their Met^Φ/N-degrons and/or AcMet^Φ/N-degrons, or whether the Arg/N-end rule pathway can target some of these proteins through their internal degrons as well.

Natural Ac/N-degrons can be repressed through steric shielding (Shemorry et al., 2013). Specifically, a protein subunit that contacts an Nt-acetylated subunit in an oligomeric complex may sequester that subunit's Ac/N-degron and thereby preclude, reversibly, its recognition by the Ac/N-end rule pathway

Arg/N-end rule pathway as well as its mouse counterparts Ubr1 and Ubr2 can recognize Met-Φ proteins through their unacetylated N-terminal Met residues (Figures 1, 2, 3, 4, 5, S3, and S4). (A Met-Φ protein bears N-terminal Met followed by a large hydrophobic [Φ] non-Met residue, i.e., Leu, Phe, Tyr, Trp or Ile.) The resulting complementarity between the Arg/N-end rule and Ac/N-end rule pathways makes possible the proteolysis-mediated control of Met-Φ proteins irrespective of the extent of their Nt-acetylation. Specifically, the Ac/N-end rule pathway can target an Nt-acetylated AcMet-Φ protein but not the otherwise identical unacetylated Met-Φ protein. The latter, however, can be destroyed as well, because it contains a Met^Φ/N-degron. This previously unknown class of N-degrons is recognized by the Ubr1-dependent Arg/N-end rule pathway. The resulting dual-pathway circuit is summarized in Figures 6 and 7B.

In either yeast or mammals, ~15% of genes encode Met-Φ proteins. For this reason alone, the present advance has signifi-

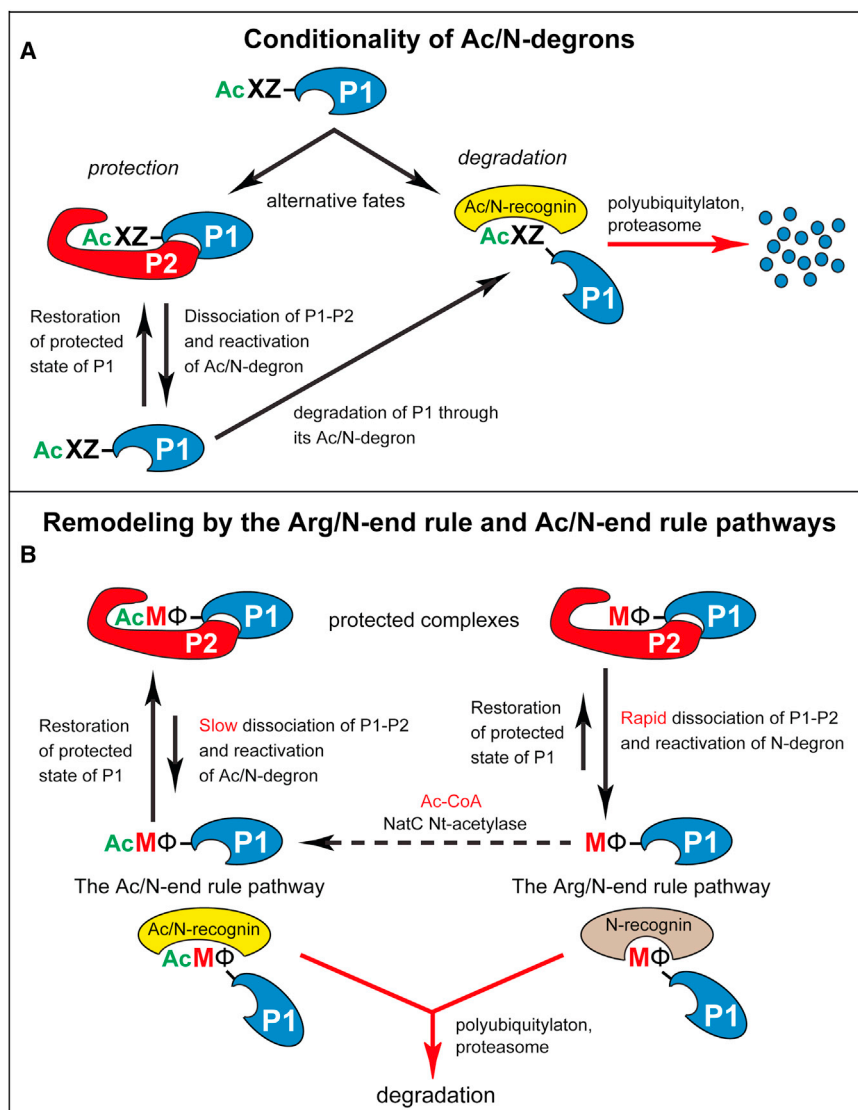


Figure 7. Conditionality of Ac/N-Degrans and Protein Remodeling by the N-End Rule Pathway

(A) Conditionality of Ac/N-degrons. This diagram summarizes the previously attained understanding of the dynamics of Nt-acetylated proteins vis-à-vis the Ac/N-end rule pathway (see [Discussion](#)), in conjunction with the initial discovery of the Ac/N-end rule pathway ([Hwang et al., 2010b](#); [Shemorry et al., 2013](#)).

(B) The recognition of unacetylated Met- Φ proteins by the Arg/N-end rule pathway and of Nt-acetylated AcMet- Φ proteins by the Ac/N-end rule pathway underlies the proposed remodeling of protein complexes. Owing to different rates of dissociation of Nt-acetylated (AcMet- Φ) versus unacetylated (Met- Φ) complexes (see [Discussion](#)), the subunit-selective degradation of the unacetylated P1 (Met- Φ) subunit of a P1-P2 complex upon its dissociation would allow the replacement-mediated conversion of P1-P2 into a similar but more stable complex containing the Nt-acetylated (AcMet- Φ) counterpart of the Met- Φ P1 subunit. To maximize generality of this description, the Nt-acetylation state of the P2 protein subunit was left unspecified, in contrast to the P1 subunit. Nt-acetylation of cellular proteins is largely cotranslational. The dashed arrow signifies the current uncertainty about rates of post-translational Nt-acetylation.

See [Discussion](#) for specific ramifications of this model. See also [Figure S1](#).

destabilization of some chloroplast DNA-encoded proteins upon a partial retention of their N-terminal Met, a finding that had not been understood in mechanistic terms ([Giglione et al., 2003](#)). Produced in bacteria-like chloroplasts of plant cells, these proteins bear, initially, the N-terminal formyl-Met (fMet) residue. We suggested that the transient (eventually

([Figures 7A and S1A](#)). For example, *S. cerevisiae* Cog1, a subunit of the COG complex, was shown to contain an Ac/N-degron. Nevertheless, Cog1 is long lived if expressed at normal (endogenous) levels. However, an overexpressed Cog1 is short lived ([Shemorry et al., 2013](#)). Moreover, the previously long-lived endogenous Cog1 becomes short lived if the production of Cog1 goes up in a cell. The cause of Cog1 destabilization was traced to the loss of stoichiometry, as only a minority of overproduced Cog1 molecules could repress their Ac/N-degrons through the binding to other, less abundant (normally expressed) subunits of the COG complex ([Shemorry et al., 2013](#)). This understanding has explained, among other things, how the prevalence of Ac/N-degrons (~90% of human proteins are Nt-acetylated, apparently irreversibly) can be consistent with the fact that most Nt-acetylated proteins are at least intermittently long lived in vivo.

The targeting of Met Φ /N-degrons and AcMet Φ /N-degrons by, respectively, the Arg/N-end rule and Ac/N-end rule pathways ([Figures 6 and 7B](#)) may also account for the previously noted

deformylated) N-terminal fMet of bacterial proteins may act as an fMet-based N-degron ([Hwang et al., 2010b](#)). Such a degradation signal would be analogous to the previously identified eukaryotic Ac/N-degrons, but with the transient formyl moiety (instead of the permanent acetyl moiety) at the N termini of nascent bacterial proteins. This possibility remains to be examined.

MF-Pre5, a subunit of the 20S proteasome, was relatively long-lived in WT, *ubr1Δ*, and *naa30Δ ubr1Δ* cells ($t_{1/2} > 1$ hr). However, in *naa30Δ* cells (lacking NatC but containing the Arg/N-end rule pathway), MF-Pre5_{ha} became so short-lived ($t_{1/2} < 30$ min) that it was barely detectable even before the chase ([Figure 5A](#)). An explanation, below, of the striking destabilization of MF-Pre5_{ha} in the absence of its Nt-acetylation is based on structural studies of Nt-acetylated proteins by Schulman, Barford and colleagues ([Monda et al., 2013](#); [Scott et al., 2011](#); [Zhang et al., 2010a](#)).

The Nt-acetylation of MF-Pre5_{ha} in WT cells ([Arnesen et al., 2009](#)) precludes its targeting by the Arg/N-end rule pathway.

The degradation of Nt-acetylated AcMF-Pre5_{ha} is slow in WT cells, in contrast to the rapid destruction of unacetylated MF-Pre5_{ha} in *naa30Δ* cells (Figure 5A). We suggest this is so because the AcMet^Φ/N-degron of Nt-acetylated AcMF-Pre5_{ha} is rapidly repressed (shielded), owing to its interactions with other subunits of the proteasome and/or with proteasomal chaperones (Matias et al., 2010; Tomko and Hochstrasser, 2013), by analogy with the efficacious repression of the previously characterized natural Ac/N-degrons, in proteins such as Cog1 and Hcn1 (Shemorry et al., 2013). However, in *naa30Δ* cells, the now unacetylated N-terminal Met of MF-Pre5_{ha} acts as an active Met^Φ/N-degron of the Arg/N-end rule pathway, resulting in the observed destruction of MF-Pre5_{ha} (Figure 5A). So far, this line of reasoning invoked concepts validated earlier, including the conditionality of Ac/N-degrons (Shemorry et al., 2013). The remaining step, described below, is to explain why the Met^Φ/N-degron of unacetylated MF-Pre5_{ha} (in *naa30Δ* cells) is much more active than the AcMet^Φ/N-degron of Nt-acetylated AcMF-Pre5_{ha} (in WT cells) (Figure 5A).

Nt-acetylation of a protein makes its initially charged N terminus uncharged, more bulky, and more hydrophobic. Schulman and colleagues have shown that the strength of cognate protein interactions that involve the Nt-acetyl group is higher, by approximately 100-fold, in the presence versus the absence of this group (Monda et al., 2013). Because MF-Pre5_{ha} is not Nt-acetylated in *naa30Δ* cells, a degron-shielding “protective” complex that contains unacetylated MF-Pre5_{ha} would still be expected to form but would be much less tight in these cells than in WT cells, which contain Nt-acetylated AcMF-Pre5_{ha}. Given the findings with other Nt-acetylated proteins (Monda et al., 2013), a significant difference in the rate of dissociation of protective complexes containing Nt-acetylated versus unacetylated MF-Pre5_{ha} is likely to account for the faster degradation of MF-Pre5_{ha} in *naa30Δ* cells (Figure 5A). This mechanism, to be verified and explored in future studies, may prove to be general and illuminating (Figure 7B).

The degradation, in *naa30Δ* cells, of the (unacetylated) MF-Pre5 proteasomal subunit by the Arg/N-end rule pathway (Figure 5A) suggested that the slow-growth phenotype of *naa30Δ* cells might be caused, in part, by low levels of MF-Pre5 in these cells. Indeed, the growth rate of *naa30Δ* cells (but not of WT cells) was significantly increased by overexpression of MF-Pre5 (Figure 5B). Thus, the slow growth of *naa30Δ* cells (which cannot Nt-acetylate Met-Φ proteins) is caused, at least in part, by abnormally low levels of unacetylated and therefore short-lived Met-Φ proteins that include MF-Pre5. These proteins are longer-lived in WT cells (owing to efficacious shielding of their Ac/N-degrons) but become vulnerable to the Arg/N-end rule pathway in the absence of Nt-acetylation (Figures 6 and 7B). In a telling sequel to this result, we also found that *naa30Δ ubr1Δ* cells that did not overexpress Pre5 grew as fast as *naa30Δ* cells that overexpressed Pre5 (Figure 5B). Thus, not only it is true that a significant part of the growth defect of *naa30Δ* cells (in which MF-Pre5 is degraded) can be rescued by overexpressing MF-Pre5, but a nearly identical extent of growth rescue can also be produced by deleting *UBR1* in the *naa30Δ* genetic background and thereby stabilizing MF-Pre5 (Figures 5A and 5B).

As discussed above, the previously characterized conditionality of Ac/N-degrons (Shemorry et al., 2013), including AcMet^Φ/N-degrons, is likely to be more pronounced than the

conditionality of Met^Φ/N-degrons, because protective complexes containing unacetylated Met-Φ subunits would dissociate more rapidly (Monda et al., 2013). If so, one function of the dual-pathway circuit in Figures 6A, 6B, and 7B is the degradation-mediated remodeling of protein complexes. This remodeling, based on the previously discovered subunit selectivity of protein degradation by the Arg/N-end rule pathway (Johnson et al., 1990), can eliminate an unacetylated Met-Φ subunit from a complex, thereby making possible the replacement of that subunit by its Nt-acetylated counterpart.

An incomplete Nt-acetylation of some newly formed proteins in WT cells stems, in part, from substoichiometric levels of ribosome-associated Nt-acetylases vis-à-vis the levels of ribosomes. A complex containing an unacetylated Met-Φ subunit instead of its cognate Nt-acetylated counterpart would be more prone to dissociation (Monda et al., 2013). Although a faster disassembly of the complex may compromise its function, it would also facilitate the repair (remodeling) of this complex through the degradation-mediated replacement of its unacetylated subunits by their Nt-acetylated counterparts. One prediction of this model is that some Met-Φ proteins may be Nt-acetylated in vivo to a lower extent than they appear to be in Nt-acetylation databases (which are based on steady-state measurements) because unacetylated versions of these proteins would be preferentially destroyed by the Arg/N-end rule pathway through their Met^Φ/N-degrons.

The conditional and processive protein degradation by the Arg/N-end rule pathway and the Ac/N-end rule pathway encompasses full-length proteins and their protein-sized fragments generated by nonprocessive proteases that include calpains, caspases, separases, secretases, and Met-aminopeptidases (Figures 6 and S1). While distinct mechanistically (they involve different N-degrons and N-recognins), the two branches of the N-end rule pathway have now been shown to interact functionally (Figures 6 and 7). One remarkable conclusion from this—still continuing—expansion of the N-end rule pathway is that nearly all 20 amino acids of the genetic code can act, in specific sequence contexts, as destabilizing N-terminal residues (N-degrons), both in their unacetylated states and after Nt-acetylation. Yet another astonishing realization, brought about by the present study and by the 2010 discovery of the Ac/N-end rule pathway (Hwang et al., 2010b; Shemorry et al., 2013), is that most proteins in a cell are conditionally short-lived N-end rule substrates, either as full-length proteins or as protease-generated fragments. Some physiological ramifications of these insights are described above, and many more remain to be explored.

EXPERIMENTAL PROCEDURES

Yeast Strains, Plasmids, and Genetic Techniques

Tables S1, S2, and S3 cite *S. cerevisiae* strains, plasmids, and PCR primers, respectively. Standard techniques were employed for strain construction and transformation. Details are described in Extended Experimental Procedures.

Purification of Sc^{Ubr1}, Mm^{Ubr1}, and Mm^{Ubr2}

The N-terminally flag-tagged *S. cerevisiae* Ubr1 (Sc^{Ubr1}), mouse Ubr1 (Mm^{Ubr1}), and mouse Ubr2 (Mm^{Ubr2}) were expressed in protease-deficient *S. cerevisiae* SC295 (Table S1) and purified by affinity chromatography as described in Extended Experimental Procedures.

SPOT Binding Assays

These assays employed a set of synthetic Met-Z-e^{K(3-10)} peptides (Z = Ala, Cys, Asp, Glu, Phe, Gly, His, Ile, Lys, Leu, Met, Asn, Pro, Gln, Arg, Ser, Thr, Val, Trp, Tyr) as well as the independently prepared Met-Leu-e^{K(3-10)} and Met-Lys-e^{K(3-10)} peptides, and their Nt-acetylated counterparts AcMet-Leu-e^{K(3-10)} and AcMet-Lys-e^{K(3-10)}. The peptides were C-terminally linked, as "dots," to a cellulose-PEG membrane in equal molar amounts. Except for varying residues at positions 1 and 2, the sequences of the 10-residue SPOT-arrayed peptides were identical to the N-terminal sequence of the extensively characterized e^K extension (see the main text). The peptides were synthesized by GmbH (JPT) (Berlin, Germany) using the JPT Peptide Technology. SPOT assays were carried out as described in [Extended Experimental Procedures](#).

Cycloheximide-Chase and Pulse-Chase Assays

They were performed largely as described ([Hwang et al., 2010b; Shemorry et al., 2013](#)). Briefly, *S. cerevisiae* strains expressing epitope-tagged test proteins were treated with cycloheximide (CHX), and the samples were processed at indicated times for protein extraction, SDS-PAGE, and immunoblotting with either anti-ha, anti-myc, or anti-tubulin antibodies. The latter antibodies were used to verify the uniformity of total protein loads. In ³⁵S-pulse-chase assays, *S. cerevisiae* were labeled with ³⁵S-methionine/cysteine for 2 to 5 min (as indicated), followed by a chase, the processing of a cell extract for immunoprecipitation with anti-ha antibody, SDS-PAGE, autoradiography, and quantification, as described in [Extended Experimental Procedures](#).

GST-Pulldown Assays

ML-e^K-GST (ML-GST) (see the main text) was expressed in *E. coli* and purified by affinity chromatography, using Glutathione HiCap Matrix (QIAGEN). The N-terminally flag-tagged full-length *S. cerevisiae* Ubr1 (Ubr1) or its flag-tagged UBR¹⁻⁷¹⁷, Ubr1^{209-1140f}, Ubr1¹⁻³¹⁰, Ubr1⁹⁸⁻⁵¹⁸, and Ubr1²⁰⁹⁻⁷¹⁷ fragments were expressed in *S. cerevisiae* SC295 ([Table S1](#)) from the P_{ADH1} promoter on a high copy plasmid. GST-pulldown assays with purified ML-GST and *S. cerevisiae* extracts containing Ubr1 or its fragments were carried out as described in [Extended Experimental Procedures](#).

Ubr1-Mediated Ubiquitylation Assay

This completely defined in vitro ubiquitylation assay comprised purified human Ub, purified *S. cerevisiae* Uba1 (the E1 enzyme), purified *S. cerevisiae* Rad6 (the E2 enzyme), purified Ubr1 (the E3 N-recognin), and purified ML-GST (see the preceding section about Ubr1 and ML-GST). Details of purification of these proteins as well as the ubiquitylation assay ([Hwang et al., 2010a](#)) are described in [Extended Experimental Procedures](#).

RT-PCR Assays

Total RNAs were extracted using RiboPure-Yeast Kit (Life Technologies) from indicated *S. cerevisiae* strains that expressed either ML-Ura3 (Ub-ML-e^K-ha-Ura3), MF-Pre5_{ha}, MI-Sry1_{ha}, or the endogenous MI-Sry1_{ha3} and were grown to A₆₀₀ of ~1 in 15 ml of SC(-Trp) or SC(-His) media containing 20 μM CuSO₄. The steps of reverse transcription, PCR amplification of resulting DNAs, and other RT-PCR procedures are described in [Extended Experimental Procedures](#).

Cell-Growth Assays

To determine whether overexpression of *PRE5* influences cell growth in specific genetic backgrounds, *S. cerevisiae* JD53 (WT), CHY371 (*naa30Δ*), and CHY372 (*naa30Δ ubr1Δ*) that carried either pCH690 (p424CUP1) or pCH1658 (p424CUP1-PRE5) were used ([Table S2](#)). Cells were grown overnight in SC-Trp medium at 30°C, then reinoculated, in triplicate, into 10 ml of SC-Trp medium in a 100 ml flask to the final A₆₀₀ of 0.2 and thereafter incubated, with rotary shaking, at 37°C for 16 hr. A₆₀₀ of cultures (each of them grown in triplicate) were measured every 4 hr. To examine effects of stressors on cell growth, JD53 (WT), JD83-1A (*ubr1Δ*), CHY371(*naa30*), or CHY372 (*naa30Δ ubr1Δ*) *S. cerevisiae* were grown in YPD medium in the presence of indicated stressors ([Figures S4G and S4H](#)), and the relative rates of cell growth were assayed as described in [Extended Experimental Procedures](#).

SUPPLEMENTAL INFORMATION

Supplemental Information includes Extended Experimental Procedures, four figures, and three tables and can be found with this article online at <http://dx.doi.org/10.1016/j.cell.2013.11.031>.

ACKNOWLEDGMENTS

We thank S.-Y. Kim (Korea Research, Institute of Biosciences and Biotechnology) for calculating the relative content of encoded human Met-Φ proteins, and D.H. Wolf (University of Stuttgart, Germany) for providing pFE15. We also thank C. Brower, K. Piatkov, J. Raskatov and B. Wadas (California Institute of Technology), and I. Hwang (Pohang University of Science and Technology) for helpful comments on the manuscript. We are grateful to members of the Hwang and Varshavsky laboratories for their assistance and advice. This work was supported by grants to C.-S.H from the National Research Foundation (NRF) of the Korea government (MSIP) (NRF-2011-0021975 and NRF-2012R1A4A1028200), the Korean Healthcare Technology R&D Project of the Ministry of Health & Welfare (H11C1279), and the T.J. Park Science Fellowship of POSCO T.J. Park Foundation, and also by grants to A.V. from the U.S. National Institutes of Health (DK039520 and GM031530). H.-K.K was supported by the Korean Government's NRF-2013-Global Ph.D. Fellowship Program (NRF-2013H1A2A1033225) and the BK21 PLUS Program.

Received: September 7, 2013

Revised: September 26, 2013

Accepted: November 20, 2013

Published: December 19, 2013

REFERENCES

- Arnesen, T., Van Damme, P., Plevoda, B., Helsens, K., Evjenth, R., Colaert, N., Varhaug, J.E., Vandekerckhove, J., Lillehaug, J.R., Sherman, F., and Gevaert, K. (2009). Proteomics analyses reveal the evolutionary conservation and divergence of N-terminal acetyltransferases from yeast and humans. *Proc. Natl. Acad. Sci. USA* 106, 8157–8162.
- Bachmair, A., Finley, D., and Varshavsky, A. (1986). *In vivo* half-life of a protein is a function of its amino-terminal residue. *Science* 234, 179–186.
- Behnia, R., Panic, B., Whyte, J.R.C., and Munro, S. (2004). Targeting of the Arf-like GTPase Arl3p to the Golgi requires N-terminal acetylation and the membrane protein Sys1p. *Nat. Cell Biol.* 6, 405–413.
- Brower, C.S., Piatkov, K.I., and Varshavsky, A. (2013). Neurodegeneration-associated protein fragments as short-lived substrates of the N-end rule pathway. *Mol. Cell* 50, 161–171.
- Choi, W.S., Jeong, B.-C., Joo, Y.J., Lee, M.-R., Kim, J., Eck, M.J., and Song, H.K. (2010). Structural basis for the recognition of N-end rule substrates by the UBR box of ubiquitin ligases. *Nat. Struct. Mol. Biol.* 17, 1175–1181.
- Dougan, D.A., Micevski, D., and Truscott, K.N. (2012). The N-end rule pathway: from recognition by N-recognins, to destruction by AAA+proteases. *Biochim. Biophys. Acta* 1823, 83–91.
- Duttler, S., Pechmann, S., and Frydman, J. (2013). Principles of cotranslational ubiquitination and quality control at the ribosome. *Mol. Cell* 50, 379–393.
- Eisele, F., and Wolf, D.H. (2008). Degradation of misfolded protein in the cytoplasm is mediated by the ubiquitin ligase Ubr1. *FEBS Lett.* 582, 4143–4146.
- Finley, D., Ulrich, H.D., Sommer, T., and Kaiser, P. (2012). The ubiquitin-proteasome system of *Saccharomyces cerevisiae*. *Genetics* 192, 319–360.
- Fredrickson, E.K., and Gardner, R.G. (2012). Selective destruction of abnormal proteins by ubiquitin-mediated protein quality control degradation. *Semin. Cell Dev. Biol.* 23, 530–537.
- Gigliione, C., Vallon, O., and Meinel, T. (2003). Control of protein life-span by N-terminal methionine excision. *EMBO J.* 22, 13–23.
- Hartl, F.U., Bracher, A., and Hayer-Hartl, M. (2011). Molecular chaperones in protein folding and proteostasis. *Nature* 475, 324–332.

- Heck, J.W., Cheung, S.K., and Hampton, R.Y. (2010). Cytoplasmic protein quality control degradation mediated by parallel actions of the E3 ubiquitin ligases Ubr1 and San1. *Proc. Natl. Acad. Sci. USA* 107, 1106–1111.
- Heinemeyer, W., Tröndle, N., Albrecht, G., and Wolf, D.H. (1994). PRE5 and PRE6, the last missing genes encoding 20S proteasome subunits from yeast? Indication for a set of 14 different subunits in the eukaryotic proteasome core. *Biochemistry* 33, 12229–12237.
- Hwang, C.-S., Shemorry, A., Auerbach, D., and Varshavsky, A. (2010a). The N-end rule pathway is mediated by a complex of the RING-type Ubr1 and HECT-type Ufd4 ubiquitin ligases. *Nat. Cell Biol.* 12, 1177–1185.
- Hwang, C.-S., Shemorry, A., and Varshavsky, A. (2010b). N-terminal acetylation of cellular proteins creates specific degradation signals. *Science* 327, 973–977.
- Johnson, E.S., Gonda, D.K., and Varshavsky, A. (1990). Cis-trans recognition and subunit-specific degradation of short-lived proteins. *Nature* 346, 287–291.
- Matias, A.C., Ramos, P.C., and Dohmen, R.J. (2010). Chaperone-assisted assembly of the proteasome core particle. *Biochem. Soc. Trans.* 38, 29–33.
- Matta-Camacho, E., Kozlov, G., Li, F.F., and Gehring, K. (2010). Structural basis of substrate recognition and specificity in the N-end rule pathway. *Nat. Struct. Mol. Biol.* 17, 1182–1187.
- Mischerikow, N., and Heck, A.J. (2011). Targeted large-scale analysis of protein acetylation. *Proteomics* 11, 571–589.
- Monda, J.K., Scott, D.C., Miller, D.J., Lydeard, J., King, D., Harper, J.W., Bennett, E.J., and Schulman, B.A. (2013). Structural conservation of distinctive N-terminal acetylation-dependent interactions across a family of mammalian NEDD8 ligation enzymes. *Structure* 21, 42–53.
- Piatkov, K.I., Brower, C.S., and Varshavsky, A. (2012a). The N-end rule pathway counteracts cell death by destroying proapoptotic protein fragments. *Proc. Natl. Acad. Sci. USA* 109, E1839–E1847.
- Prasad, R., Kawaguchi, S., and Ng, D.T.W. (2010). A nucleus-based quality control mechanism for cytosolic proteins. *Mol. Biol. Cell* 21, 2117–2127.
- Scott, D.C., Monda, J.K., Bennett, E.J., Harper, J.W., and Schulman, B.A. (2011). N-terminal acetylation acts as an avidity enhancer within an interconnected multiprotein complex. *Science* 334, 674–678.
- Setty, S.R.G., Strohlic, T.I., Tong, A.H.Y., Boone, C., and Burd, C.G. (2004). Golgi targeting of ARF-like GTPase Arl3p requires its N α -acetylation and the integral membrane protein Sys1p. *Nat. Cell Biol.* 6, 414–419.
- Shemorry, A., Hwang, C.-S., and Varshavsky, A. (2013). Control of protein quality and stoichiometries by N-terminal acetylation and the N-end rule pathway. *Mol. Cell* 50, 540–551.
- Starheim, K.K., Gevaert, K., and Arnesen, T. (2012). Protein N-terminal acetyltransferases: when the start matters. *Trends Biochem. Sci.* 37, 152–161.
- Summers, D.W., Wolfe, K.J., Ren, H.Y., and Cyr, D.M. (2013). The Type II Hsp40 Sis1 cooperates with Hsp70 and the E3 ligase Ubr1 to promote degradation of terminally misfolded cytosolic protein. *PLoS ONE* 8, e52099.
- Takatsume, Y., Ohdate, T., Maeta, K., Nomura, W., Izawa, S., and Inoue, Y. (2010). Calcineurin/Crz1 destabilizes Msn2 and Msn4 in the nucleus in response to Ca(2+) in *Saccharomyces cerevisiae*. *Biochem. J.* 427, 275–287.
- Tasaki, T.S., Sriram, S.M., Park, K.S., and Kwon, Y.T. (2012). The N-end rule pathway. *Annu. Rev. Biochem.* 81, 261–289.
- Theodoraki, M.A., Nillegoda, N.B., Saini, J., and Caplan, A.J. (2012). A network of ubiquitin ligases is important for the dynamics of misfolded protein aggregates in yeast. *J. Biol. Chem.* 287, 23911–23922.
- Tomko, R.J., Jr., and Hochstrasser, M. (2013). Molecular architecture and assembly of the eukaryotic proteasome. *Annu. Rev. Biochem.* 82, 415–445.
- Turner, G.C., and Varshavsky, A. (2000). Detecting and measuring cotranslational protein degradation in vivo. *Science* 289, 2117–2120.
- Varshavsky, A. (2008). Discovery of cellular regulation by protein degradation. *J. Biol. Chem.* 283, 34469–34489.
- Varshavsky, A. (2011). The N-end rule pathway and regulation by proteolysis. *Protein Sci.* 20, 1298–1345.
- Wada, M., Nakamori, S., and Takagi, H. (2003). Serine racemase homologue of *Saccharomyces cerevisiae* has L-threo-3-hydroxyaspartate dehydratase activity. *FEMS Microbiol. Lett.* 225, 189–193.
- Wang, F., Durfee, L.A., and Huibregtse, J.M. (2013). A cotranslational ubiquitination pathway for quality control of misfolded proteins. *Mol. Cell* 50, 368–378.
- Xia, Z., Webster, A., Du, F., Piatkov, K., Ghislain, M., and Varshavsky, A. (2008). Substrate-binding sites of UBR1, the ubiquitin ligase of the N-end rule pathway. *J. Biol. Chem.* 283, 24011–24028.
- Xiao, Q., Zhang, F., Nacev, B.A., Liu, J.O., and Pei, D. (2010). Protein N-terminal processing: substrate specificity of *Escherichia coli* and human methionine aminopeptidases. *Biochemistry* 49, 5588–5599.
- Yewdell, J.W., Lacsina, J.R., Rechsteiner, M.C., and Nicchitta, C.V. (2011). Out with the old, in with the new? Comparing methods for measuring protein degradation. *Cell Biol. Int.* 35, 457–462.
- Zhang, Z., Kulkarni, K., Hanrahan, S.J., Thompson, A.J., and Barford, D. (2010a). The APC/C subunit Cdc16/Cut9 is a contiguous tetratricopeptide repeat superhelix with a homo-dimer interface similar to Cdc27. *EMBO J.* 29, 3733–3744.